

2011

Reconfigurable optical power splitter/combiner based on Opto-VLSI processing

Haithem A. Mustafa
Edith Cowan University

Feng Xiao
Edith Cowan University

Kamal Alameh
Edith Cowan University

Follow this and additional works at: <https://ro.ecu.edu.au/ecuworks2011>



Part of the [Physical Sciences and Mathematics Commons](#)

[10.1364/OE.19.021890](https://doi.org/10.1364/OE.19.021890)

This paper was published in Optics Express and is made available as an electronic reprint with the permission of OSA. The paper can be found at the following URL on the OSA website: <http://dx.doi.org/10.1364/OE.19.021890>. © 2011 Optical Society of America. One print or electronic copy may be made for personal use only. Systematic reproduction and distribution, duplication of any material in this paper for a fee or for commercial purposes, or modifications of the content of this paper are prohibited.

This Journal Article is posted at Research Online.

<https://ro.ecu.edu.au/ecuworks2011/170>

Reconfigurable optical power splitter/combiner based on Opto-VLSI processing

Haithem Mustafa,* Feng Xiao, and Kamal Alameh

Electron Science Research Institute, Edith Cowan University, Joondalup, WA 6027, Australia
*h.mustafa@ecu.edu.au

Abstract: A novel 1×4 reconfigurable optical splitter/combiner structure based on Opto-VLSI processor and 4-f imaging system with high resolution is proposed and experimentally demonstrated. By uploading optimized multicasting phase holograms onto the software-driven Opto-VLSI processor, an input optical signal is dynamically split into different output fiber ports with user-defined splitting ratios. Also, multiple input optical signals are dynamically combined with arbitrary user-defined weights.

©2011 Optical Society of America

OCIS codes: (060.2330) Fiber optics communications; (230.1360) Beam splitters.

References and links

1. A. Queller, "Dynamic power distribution in PON/FTTP networks," *Lightwave* **21**(7), 29–31 (2004)
<http://www.lightwaveonline.com/about-us/lightwave-issue-archives/issue/dynamic-power-distribution-in-ponfttp-networks-53906787.html>.
2. M. D. Vaughn, D. Kozischek, D. Meis, A. Boskovic, and R. E. Wagner, "Value of reach-and-split ratio increase in FTTH access networks," *J. Lightwave Technol.* **22**(11), 2617–2622 (2004).
3. D. V. Thourhout, P. Bernasconi, B. Miller, W. Yang, L. Zhang, N. Sauer, L. Stulz, and S. Cabot, "Novel Geometry for an Integrated Channel Selector," *IEEE J. Sel. Top. Quantum Electron.* **8**(6), 1211–1214 (2002).
4. F. Xiao, B. Juswardy, K. Alameh, and Y. T. Lee, "Novel broadband reconfigurable optical add-drop multiplexer employing custom fiber arrays and Opto-VLSI processors," *Opt. Express* **16**(16), 11703–11708 (2008).
5. P. Bernasconi, C. R. Doerr, C. Dragone, M. Cappuzzo, E. Laskowski, and A. Paunescu, "Large N×N waveguide grating routers," *J. Lightwave Technol.* **18**(7), 985–991 (2000).
6. N. Kikuchi, Y. Shibata, H. Okamoto, Y. Kawaguchi, S. Oku, H. Ishii, Y. Yoshikuni, and Y. Tohmori, "Monolithically integrated 64-channel WDM channel selector with novel configuration," *Electron. Lett.* **38**(7), 331–332 (2002).
7. J. Capmany, B. Ortega, D. Pastor, and S. Sales, "Discrete-Time Optical Processing of Microwave signals," *J. Lightwave Technol.* **23**(2), 702–723 (2005).
8. J. Capmany, B. Ortega, and D. Pastor, "A Tutorial on Microwave Photonic Filters," *J. Lightwave Technol.* **24**(1), 201–229 (2006).
9. R. A. Minasian, K. E. Alameh, and E. H. W. Chan, "photonic based interference mitigation filters," *IEEE Trans. Microw. Theory Tech.* **49**(10), 1894–1899 (2001).
10. F. Xiao, B. Juswardy, and K. Alameh, "Tunable photonic microwave filters based on Opto-VLSI processors," *IEEE Photon. Technol. Lett.* **21**(11), 751–753 (2009).
11. T. Sugiyama, M. Suzuki, and S. Kubota, "An Integrated Interference Suppression Scheme with an Adaptive Equalizer for Digital Satellite Communication Systems," *IEICE Trans. Commun. E* **79-B**(2), 191–196 (1996).
12. P. S. Mudhar, D. A. H. Mace, J. Singh, M. A. Fisher, and M. J. Adams, "Active optical combiner switch," *IEE Proceedings-J.* **139**(1), 79–82 (1992).
13. F. Ratovelomanana, N. Vodjdani, A. Enard, G. Glastre, D. Rondi, and R. Blondeau, "Active Lossless Monolithic One-by-Four Splitters/Combiners Using Optical Gates on InP," *IEEE Photon. Technol. Lett.* **7**(5), 511–513 (1995).
14. Z. Yun, L. Wen, C. Long, L. Yong, and X. Qingming, "A 1×2 Variable Optical Splitter development," *J. Lightwave Technol.* **24**(3), 1566–1570 (2006).
15. S. S. Choi, J. P. Donnelly, S. H. Groves, R. E. Reeder, R. J. Bailey, P. J. Taylor, A. Napoleone, and W. D. Goodhue, "All-active InGaAsP-InP optical tapered-amplifier 1×N power splitters," *IEEE Photon. Technol. Lett.* **12**(8), 974–976 (2000).
16. X. Zhao and S. Jose, "Dynamic power optical splitter," Patent No US 7 068 939 B2, June 2006.
17. R. Zheng, Z. Wang, K. E. Alameh, and W. A. Crossland, "An Opto-VLSI Reconfigurable Broad-Band Optical Splitter," *IEEE Photon. Technol. Lett.* **17**(2), 339–341 (2005).

18. H. A. B. Mustafa, F. Xiao, and K. Alameh, "Adaptive Optical Splitter employing an Opto-VLSI processors and 4-f Imaging System," *J. Lightwave Technol.* **28**(19), 2761–2765 (2010).
 19. F. Xiao, K. Alameh, and T. T. Lee, "Opto-VLSI-based tunable single-mode fiber laser," *Opt. Express* **17**(21), 18676–18680 (2009).
 20. S. T. Ahderom, M. Raisi, K. Alameh, and K. Eshraghian, "Testing and Analysis of Computer Generated Holograms for MicroPhotonics Devices," in *Proceeding of the second IEEE international Workshop on Electronic design, Test and applications (DELTA'04)*, Perth, Australia, Jan. 28–30, 2004, pp. 47–52.1.
-

Introduction

Recently, reconfigurable optical power splitters/combiners have attracted much attention due to the rapid deployment of passive optical networks (PON) for fiber-to-the-premises (FTTP), optical metropolitan area networks (MAN), and active optical cables for TV/video signal transport and distribution [1]. Currently, passive optical splitters/combiners are used in PONs where several hundred users share one optical line terminal (OLT) at the central office, distributing optical power to several tens of optical network units (ONUs) at the customer end of the network, each of which is shared by many users [2]. However, passive optical power splitters/combiners have limitations, not only in adding/dropping users to/from an ONU but also in changing services for each user [3–6]. A reconfigurable optical power splitter/combiner can dynamically distribute/combine the optical power and services to/from users in the entire optical access network, thus providing numerous advantages such as improvement of optical network efficiency and network scalability, and high network reliability.

Another possible application of reconfigurable optical splitters/combiners is in the area of photonic signal processing [7, 8], where lightweight and broadband are of prime concern [9–11]. A reconfigurable optical splitter/combiner provides RF photonic systems with the capability of dynamically changing the weights of optical signals leading to adaptive signal processing.

Not many dynamic optical splitter/combiner structures have previously been reported [12, 13], and none of the reported dynamic optical splitter structures [14–18] have demonstrated the capability of combing optical beams dynamically. In particular, the proof-of-principle 1×2 adaptive optical splitter based on Opto-VLSI processor reported by the authors [18] has low resolution and limited output port counts due to the difficulty in controlling the beam waist.

In this paper, we propose a novel reconfigurable optical splitter/combiner structure employing an Opto-VLSI processor and a 4-f imaging system with an optimized optical beam waist profile, enabling high-resolution optical power splitting to a larger number of output optical ports. The new adaptive optical splitter/combiner has additional advantages including (i) both optical signal splitting and combining are achieved through software using the same structure, (ii) high diffraction efficiency (i.e. lower optical loss) as more pixels are covered by the input optical beams, (iii) low inter-port crosstalk, (iv) simple user interface, and (v) compressed hardware and compact packaging. A computer program was especially developed to drive the Opto-VLSI processor and generate the desired phase holograms that split an input signal arbitrarily and accurately to multiple output optical fiber ports, and also combine multiple input signals with arbitrary weights into a single output optical fiber port.

2. Opto-VLSI processors and optical beam multicasting

The Opto-VLSI processor is an electronically-driven diffractive element capable of steering/shaping an incident optical beam without mechanically moving parts. As shown in Fig. 1, an Opto-VLSI processor comprises an array of liquid crystal (LC) cells driven by a Very-Large-Scale-Integrated (VLSI) circuit [17, 18], which generates digital holographic diffraction gratings that achieve arbitrary beam deflection/multicasting. A transparent Indium-Tin Oxide (ITO) layer is used as the ground electrode, and a quarter-wave-plate (QWP) layer is deposited between the LC and the aluminum mirror to accomplish

polarization-insensitive operation. The voltage level of each pixel can individually be controlled by using a few memory elements that select a discrete voltage level and apply it, through the electrodes, across the LC cell.

A multicasting phase hologram can split an incident optical beam to N output beams with variable intensities in different directions, as illustrated in Fig. 1. A collimated beam incident onto the Opto-VLSI processor is diffracted along different directions, where the power of each diffracted beam depends on the multicasting phase hologram. The beam multicasting resolution, or minimum splitting angle relative to the zeroth order diffraction beam, is given by [19]

$$\alpha = \arcsin\left(\frac{\lambda}{N \times d}\right) \quad (1)$$

where λ is the optical wavelength, N denotes the number of pixels illuminated by the incident optical beam, and d is the pixel pitch.

Several computer algorithms, such as the genetic, simulated annealing, phase encoding, and projection algorithms [20], have been used for generating optimized multicasting phase holograms that produce a target far-field distribution, defined by the replay beam positions and the corresponding power splitting ratios. For a target multicasting profile, an optimised phase hologram can always be synthesized, which minimizes the 0th order diffraction and the crosstalk at every output port.

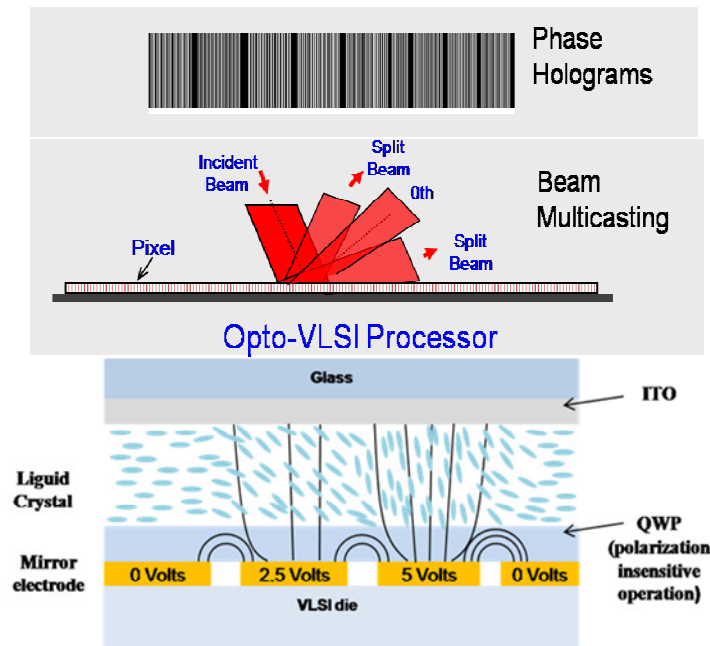


Fig. 1. The top figure illustrates the capability of the Opto-VLSI processor to perform optical beam multicasting through phased holograms. The bottom figure illustrates the phase modulation of the light through the application of voltage across the liquid crystal cells.

3. Experiments

3.1. System description

The structure of the proposed reconfigurable optical power splitter/combiner is shown, through an experimental setup, in Fig. 2. It consists of an Opto-VLSI processor, a lens, and an optical fiber array, aligned to form a 4-f imaging system. The Opto-VLSI processor has

1×4096 pixels with pixel size of 1.0 μm wide and 6.0 mm length, and 1.8μm pixel pitch (i.e. 0.8 μm of dead space between pixels). To demonstrate the 1×4 adaptive optical splitter, a custom-made fiber array with spacing 127 μm was used. The spacing between the output ports was 254 μm (twice of the fiber array spacing), thus the split beam angles were $\theta = \pm 0.58, \pm 1.16$ with respect to 0th order beam direction, as illustrated in Fig. 2. The power of the 0th order beam was coupled to a fiber port for monitoring the diffraction efficiency of the Opto-VLSI processor.

A 1550 nm laser source with an output optical power of +1.5 dBm was used as the input signal, and launched through the input port of the splitter. A lens of focal length $f = 25$ mm was placed between and at an equal distance, f , from both the fiber array and the Opto-VLSI processor. With no phase hologram uploaded onto the Opto-VLSI processor, only the 0th order diffraction beam was reflected back and focused through the imaging system into same fiber input port 5 centered the four output fiber ports, resulting in minimum crosstalk into ports 2, and 3, as illustrated in Fig. 2. The 0th order signal was directed to optical spectrum analyzers (OSA), via a circulator, in order to monitor the diffraction efficiency. The input signal from the input port at the fiber array was collimated through a lens, to an optical beam diameter of 5.48 mm, which illuminated around 3046 pixels of the Opto-VLSI processor, leading to a high diffraction efficiency and high optical splitting resolution of 0.01 degree (around 10 times better than the resolution reported in [18]).

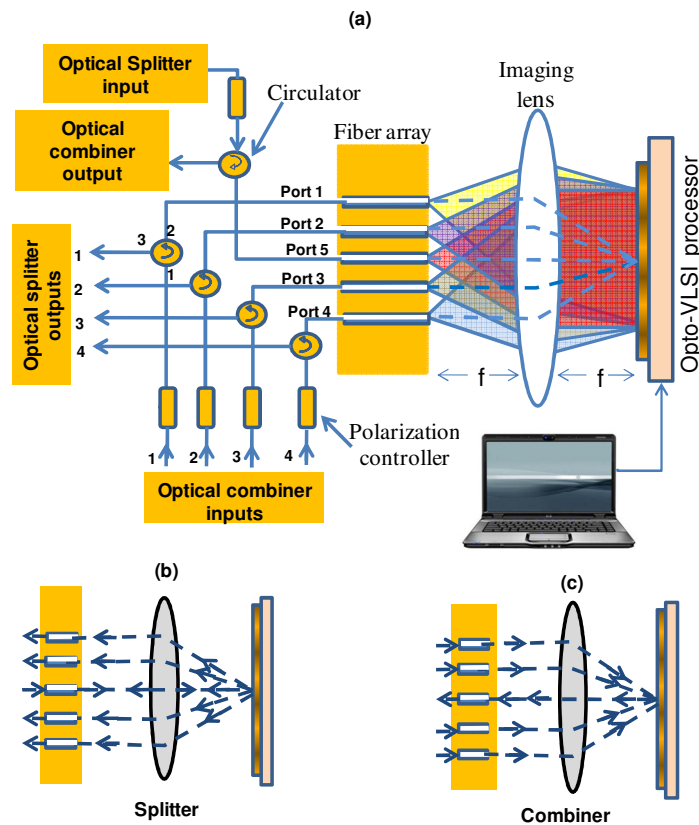


Fig. 2. (a) Schematic diagram of the reconfigurable optical splitter/combiner using an Opto-VLSI processor and a 4- f imaging systems. (b) and (c) Optical beam propagation for splitting and combining modes, respectively.

By driving the Opto-VLSI processor with an optimized multicasting phase hologram, the optical beam illuminating the Opto-VLSI processor was split into four different optical

beams (in addition to the 0th order beam) which propagated along the optimized directions so that they were coupled back into the fiber output ports through the 4-f imaging system. The split optical beams coupled into the output ports propagated along angles equal to $\theta_{2,3} = \pm 0.58^\circ$, and $\theta_{1,4} = \pm 1.16^\circ$ with respect to the 0th order beam direction. Optical spectrum analyzers (OSA) were used to monitor the power levels of the split optical signals coupled into the output ports 1, 2, 3 and 4.

To demonstrate the principle of the reconfigurable optical combiner, four optical signals of equal power levels (-5.7dBm) were launched into Ports 1, 2, 3 and 4 as in Fig. 2, and, through a multicasting phase hologram, combined into Port 5, which was monitored using an optical spectrum analyzer. As will be discussed subsequently, a multicasting phase hologram uploaded onto the Opto-VLSI processor enabled the four optical signals launched into Ports 1-4 to be combined at Port 5 with a weight profile that matches the splitting profile of the corresponding multicasting phase hologram.

3.2. Experimental Results and Discussion

Several scenarios with different splitting ratios were attempted in the experiments to demonstrate the reconfigurable optical power splitting/combining capability of the proposed optical splitter/combiner. Table 1 shows the measured output power levels, P₁, P₂, P₃ and P₄ of the splitter, coupled into Port 1, Port 2, Port 3 and Port 4, respectively, corresponding to different splitting ratios (H).

As shown in Table.1, in Scenario 1 a multicasting hologram corresponds to a splitting profile H1 = 1.0:1.0:1.0:1.0 was used, demonstrating that the input optical power is split equally into the four output ports, resulting in uniform optical power distribution at all the four output ports. In Scenarios 2, a splitting profile H2 = 1.0:1.0:0.01:1.0 was used, which corresponds to the case when the output signal in Port 3 was attenuated by 20 dB. In Scenario 3, the signals coupled to Port 2 and Port 3 were switched off by uploading a phase hologram corresponding to a splitting ratio of H3 = 1.0:0.0:0.0:1.0, respectively. The measured crosstalk level was around -30 dB. In Scenario 4 the output optical signals coupled to Port 2 and Port 3 were attenuated by 3 dB corresponding to a splitting profile of H4 = 1.0:0.5:0.5:1.0.

Table 1. Different splitting profiles corresponding to optimised multicasting holograms uploaded onto the Opto-VLSI processor, and the corresponding measured output optical power levels at Ports 1-4

Splitting ratio	P 1 (dBm)	P 2 (dBm)	P 3 (dBm)	P 4 (dBm)
H1 = 1.0:1.0:1.0:1.0	-13.18	-13.47	-13.37	-13.76
H2 = 1.0:1.0:0.01:1.0	-13.16	-13.47	-33.01	-12.59
H3 = 1.0:0.0:0.0:1.0	-11.87	-42.50	-43.93	-11.54
H4 = 1.0:0.5:0.5:1.0	-12.30	-16.60	-16.83	-12.10

Figure 3(a) shows the measured optical power coupled into the four output ports when the output power coupled into Port 1 was varied while keep the power levels at Port 2, Port 3, and Port 4 were kept constant. It is obvious from Fig. 3(a) that arbitrary output power splitting ratio can be attained for an output port while keeping the optical power at the other ports unchanged. The measured maximum output power uniformity for the fixed-weight output ports (2, 3 and 4) was less than 2 dB. Figure 3(b) shows the measured optical power levels coupled into the output fiber ports while the splitting ratios for both Port 1 and Port 4 were varied while keeping the splitting ratios for Port 2 and Port 3 fixed. The measured maximum output power fluctuation for the fixed-weight output ports was also around 2 dB.

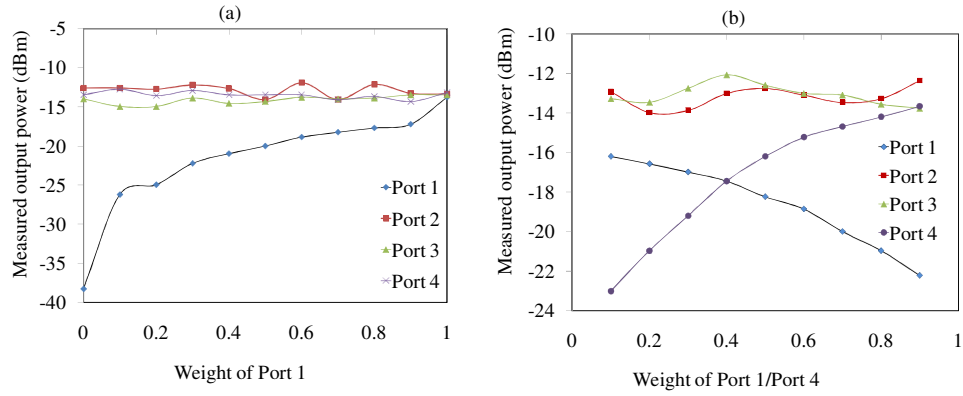


Fig. 3. (a) Measured optical power coupled into the output fiber Ports when varying the weight of Port 1 while keeping the splitting ratios for others output fiber ports constant. (b) Measured optical power coupled into the output fiber Ports when varying the weights of Port 1 and Port 4 while keeping the splitting ratios for Port 2 and Port 3 weights unchanged.

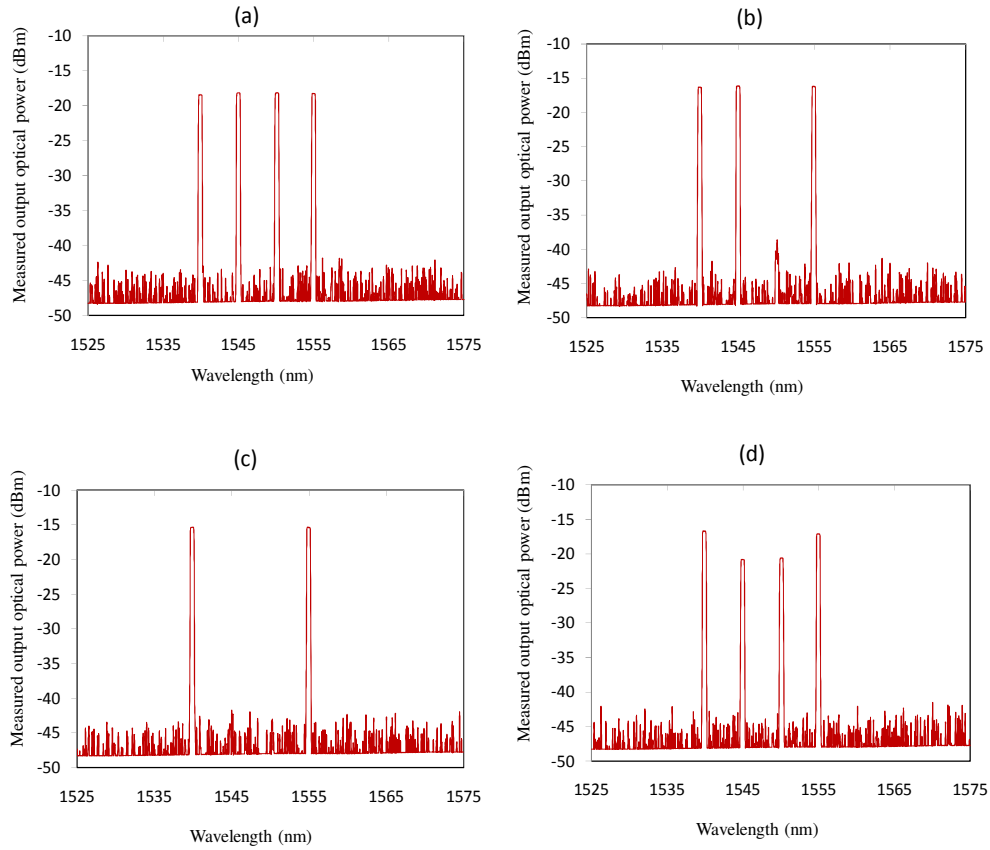


Fig. 4. Input signals launched into Ports 1, 2, 3, and 4, and output combined optical signal at Port 5 for phase holograms corresponding to splitting ratios of (a) 1.0:1.0:1.0:1.0, (b) 1.0:1.0:0.01:1.0, (c) 1.0:0.0:0.0:1.0 and (d) 1.0:0.5:0.5:1.0.

Figures 3(a, b) demonstrates the ability of the reconfigurable optical splitter structure to realize arbitrary optical splitting ratios through the use of optimized multicasting phase holograms.

The principle of the reconfigurable optical combiner was demonstrated by launching four input signals into Ports 1, 2, 3 and 4 and measuring the output signal from Port 5. Figures 4(a-d) show the output combined optical signal at Port 5 for the same phase holograms used in Table.1, which correspond to combining profiles of 1.0:1.0:1.0:1.0, 1.0:1.0:0.01:1.0, 1.0:0.0:0.0:1.0 and 1.0:0.5:0.5:1.0, respectively. Note that in Fig. 4(d) the power levels of the two center channels are actually around 4 dB below those of the outside channels, as evident from Table 1, row 4. The discrepancy between theory and experimental measurements is attributed to measurement errors. Figures 4(a-d) demonstrates the ability of the Opto-VLSI processor to combine the input optical signals with an arbitrarily weight profile and couple them into the output fiber Port 5.

Figures 3 and 4 demonstrate the ability of the reconfigurable optical splitter/combiner structure to realize arbitrary optical splitting/combining ratios through the use of optimized multicasting phase holograms. The measured output power splitting/combining ratios are in excellent agreement with the user defined ratios. Note that the crosstalk for dynamic splitting/combining is around -30 dB.

To investigate the spectral bandwidth of the proposed adaptive optical splitter/combiner, a broadband light source with spectra range from 1525nm to 1575nm was used at the input fiber port (Port 5). The measured optical spectra at Ports 1-4 are shown in Fig. 5, for a splitting ratio equal to 1.0:1.0:1.0:1.0. The measured maximum output power fluctuation for the four output ports was around 2.0 dB over a wavelength span from 1525 to 1570 nm, demonstrating a splitter bandwidth in excess of 40 nm.

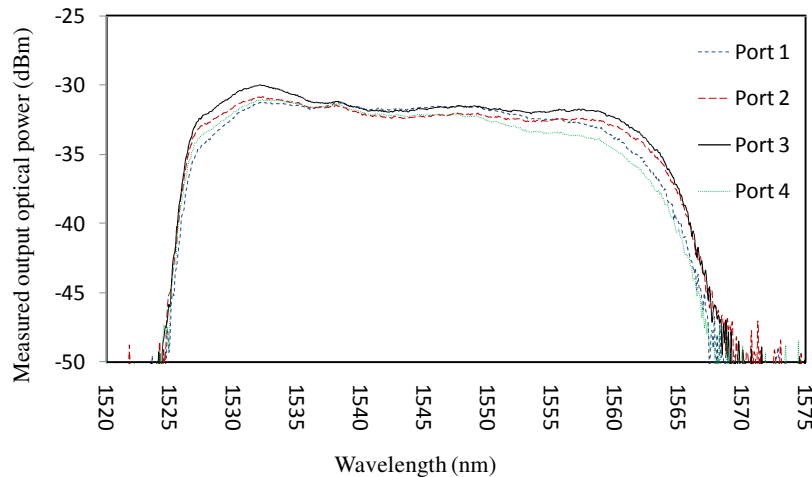


Fig. 5. Measured optical spectra at Ports 1-4 of the reconfigurable optical splitter for a uniform splitting profile of 1.0:1.0:1.0:1.0. Input signal launched at Port 5 is the Amplified Spontaneous Emission (ASE) of an Erbium-Doped Fiber Amplifier (EDFA).

The total insertion loss of the reconfigurable optical power splitter was 5 dB, to which the Opto-VLSI processor contributed around 3 dB due to the low fill factor of the Opto-VLSI processor. The 4-f imaging system alignment, optical circulator, and imperfect optical components used in the experiments contributed the remaining 2 dB of insertion loss. For the reconfigurable optical power combiner, an additional 6 dB loss was measured (or a factor of 4) which is due to the inherent signal multicasting (1:4 splitting ratio). The total insertion loss can further be reduced through an improved Opto-VLSI chip design i.e. reducing the dead

area between pixels to below 0.25 micron, and the use of broadband AR coatings for the various optical components.

4. Conclusion

A 1×4 reconfigurable optical splitter/combiner structure employing an Opto-VLSI processor in conjunction with a 4-f imaging system has been demonstrated. Experimental results have shown that an input optical signal can arbitrarily be split and coupled into four output optical fiber ports by simply uploading optimized multicasting phase holograms onto the Opto-VLSI processor. The experimental results have also demonstrated that four input optical signals can dynamically be combined with arbitrary weights into a single optical fiber port. A crosstalk level below -30 dB and a wavelength range exceeding 40 nm have experimentally been measured, making the reconfigurable optical splitter/combiner attractive for access optical networks and optical signal processing.

Acknowledgment

We acknowledge the support of the Faculty of Computing, health and Science, Edith Cowan University, Department of Nanobio Materials and Electronics, Gwangju Institute of science and Technology, Korea, and the State Key Laboratory of Advanced Optical Communication Systems and Networks, China.